Magnetic-Resonance Evaluation of the Suitability of Microstructured Polymer Optical Fibers As Sensors for Ionic Aqueous Solutions

Felicity M. Cox,[†] Konstantin I. Momot,[*,‡] and Philip W. Kuchel[§]

Optical Fibre Technology Centre and School of Molecular and Microbial Biosciences, University of Sydney, New South Wales 2006, Australia, and School of Physical and Chemical Sciences, Queensland University of Technology, GPO Box 2434, Brisbane, Queensland 4001, Australia

ABSTRACT Nuclear magnetic resonance was used to probe the distribution of water and ionic species in a microstructured poly(methyl methacrylate) (PMMA) polymer optical fiber (MPOF), with a plan to assess the suitability of these fibers for aqueous chemosensing. The NMR spectra and the measurements of proton spin relaxation in hydrated fibers demonstrated the presence of two distinct pools of water: water residing in the microstructure channels and the hydration water residing in the polymer matrix of the fiber. No facile chemical exchange between these two pools was present. The NMR peaks of the two pools of water were separated by 1.53 ppm. Relaxation measurements of the fiber samples doped with aqueous copper sulfate showed that charged ions freely entered the microstructure channels but were completely excluded from the polymer matrix of the fiber. Measurements of the apparent diffusion coefficient of water along the axial direction of the fiber showed that water molecules moved unimpeded along the channels. This is the first reported magnetic-resonance study of microstructured optical fibers. The findings suggest that microstructured PMMA fibers are compatible with ionic aqueous solutions and could provide a robust and durable platform for chemical-sensing applications.

KEYWORDS: Polymer optical fibers • fiber optics sensors • NMR characterization of materials • paramagnetic relaxation • PGSE diffusion NMR • hydrated PMMA

INTRODUCTION

Microstructured optical fibers consist of a solid matrix with a series of hollow channels running along the length of the fiber (1). They can be used to guide light in either the solid matrix or the hollow core of the fiber. The diameter of the channels can be in the range from 1 to 60 μm. Microstructured optical fibers provide an excellent platform for optical chemosensors because of the large overlap between the optical field and analyte introduced into the channels. Microstructured optical fiber sensors have been used to detect a variety of analytes including gases (2, 3), aqueous solutions (4, 5), and binding events involving biochemical species (6).

Microstructured polymer optical fibers (MPOFs) (7) are microstructured optical fibers made from a polymer. Poly(methyl methacrylate) (PMMA) is the most common choice of the polymer, but other materials have also been used (8). MPOF sensors present some advantages over their silica counterparts, including the ease of surface functionalization and suitability for in vivo use (4−6, 8). Here, we report on the distribution of the absorbed water and the distribution of an ionic species (Cu^{2+}) within a PMMA MPOF. We discuss the findings in the context of potential chemical-sensing applications involving ionic solutions.

The performance of MPOFs in optical sensing applications depends on a wide range of factors that characterize the interaction between the fiber, the analyte, and the optical field. Reliable use of MPOFs requires a detailed understanding of their properties in aqueous environments. Besides the microstructure channels, the polymeric material forming the matrix of the fiber can itself be thought of as a nanoporous media: many Angstrom- or nanometre-sized molecules can permeate the polymer chain meshwork (9). PMMA is capable of absorbing both water (10, 11) and organic solvents (12, 13). A water content of 2.1% (wt/wt) in fully hydrated PMMA at room temperature has been reported (14). The transport of organic and inorganic solutes through the PMMA matrix has been used to introduce dopants into MPOFs (13). The absorption of the solutes is determined mainly by their molecular size, charge, the chemistry of the polymer, and the density of the polymeric network comprising the matrix. The distribution and exchange of analyte solutes between the PMMA matrix and the channels determine the suitability of the fiber for a particular sensing application. The ease of exchange of solutes between the matrix and the ambient solution can also determine whether a fiber-based sensor is reuseable. Surface interactions at the polymer/channel interface are another factor that can affect sensor performance. Such interactions can be due to, for example, the electric double layer (15) or the adsorption of solute molecules at the PMMA/water interface. Finally, sensor perfor-

* Corresponding author. E-mail: k.momot@qut.edu.au. Fax: 61 7 3138 1521.
Received for review September 17, 2008 and accepted November 30, 2008
[†] Optical Fibre Technology Centre, University of Sydney.
[‡] Queensland University of Technology.
[§] School of Molecular and Microbial Biosciences, University of Sydney.
DOI: 10.1021/am800059c

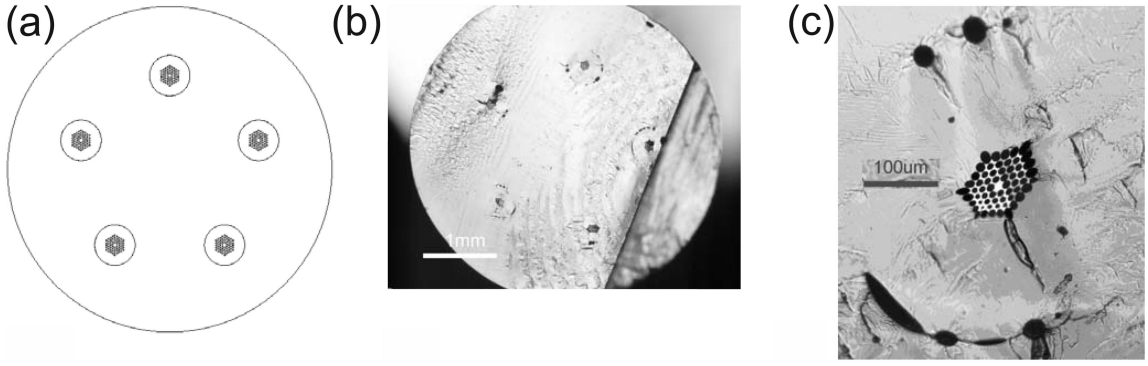

FIGURE 1. Microstructured PMMA optical fibers: (a) schematic representation of the cross-section of the fiber; (b) micrographic image of a typical MPOF sample; (c) a single microstructured region of a typical sample. As explained in Materials and Methods, the fiber samples used in this study were manufactured with five microstructure regions in order to maximize the NMR signal from channel water.

mance can be affected by the presence of restrictions to capillary flow in MPOF channels.

In this work, we used NMR relaxation and line shape measurements to study the distribution of water between the microstrucutre channels and the polymer matrix. Exchange of water between the two compartments was investigated. NMR relaxation measurements were also used to study the distribution of Cu^{2+} ions between the channels and the polymer matrix. Cu^{2+} species was chosen because of its well-characterized relaxivity in aqueous solutions (16, 17). Finally, the self-diffusion coefficient of water in the direction of the axis of the fiber was measured with the aim of ascertaining, whether restrictions were present to the axial diffusion along the microstructure channels. The results show that the analyte solution entered the microstructure channels unimpeded; the PMMA matrix of the fibers was hydrated; and the ionic species were confined to the microstructure channels of the fiber. Exclusion of ionic species from the polymer matrix suggests that microstructured PMMA optical fibers could provide a robust and durable platform for chemical-sensing applications involving ionic species.

MATERIALS AND METHODS

Sample Fabrication. Two types of samples were investigated: polymer samples without microstructure, which are referred to as blank samples, and microstructured fibers. The blank samples were prepared from optical-grade PMMA obtained from Vink B. V. (Baarn, The Netherlands) and were drawn down to an outer diameter of 4 mm using a procedure described previously (18). The blank samples were used for comparison with the microstructured samples in hydration and doping experiments, which are described below. The blank samples were also used for the measurement of the density of PMMA, degree of hydration and the diffusion coefficient of hydration water in PMMA.

The microstructured fibers were prepared from optical-grade PMMA obtained from Röhm GmbH (Darmstadt, Germany). NMR relaxation measurements discussed below show that the differences between the hydration state of the two batches of PMMA were not significant. The MPOF samples were fabricated using a previously reported procedure (18) with some modifications. The modifications of the standard procedure consisted of: (1) using five microstructure regions rather than one, and (2) drawing the fibers down to the outer diameter of 4 mm rather than 250 μm. These modifications were made with the aim of making the fiber samples more amenable to NMR measurements. A schematic diagram of the final sample and typical optical microscopic images are shown in Figure 1. For the NMR measurements, the fibers were cut into samples 2−3 cm in length.

Sample Hydration and Doping. Water used for sample hydration or doping was obtained from a Milli-Q reverse-osmosis apparatus (Millipore, Bedford, MA). Copper sulfate pentahydrate ($CuSO_4 \cdot 5H_2O$) was used to prepare aqueous $CuSO_4$ solutions at concentrations of 0.25, 2.0, and 4.0 mM. The microstructured optical fiber samples were hydrated by being placed in water for at least 20 days, which ensured a >96% complete hydration of the polymer. Doping of the samples was achieved by placing them in a $CuSO_4$ solution of the required concentration for the same length of time. Hydration and doping of the blank PMMA samples was achieved using an identical procedure.

Following the 20-day period, the samples were removed from the solutions (or from water). The outside of the samples was wiped dry using Kimwipe tissues. This removed the water not absorbed by the samples but did not affect the hydration state of the PMMA matrix or the microstructure channels. Samples thus prepared were used for the NMR measurements.

Optical Microscopy. Microscopic images were obtained from the whole (nonsectioned) samples using a Nikon Eclipse ME600 microscope equipped with a camera (Nikon DXM1200F). An unpolarized, white light source was used. The digital resolution of the images was $(1.2\ \mu m)^2$.

Hydration Measurements. The ingress of water into PMMA was used to measure the equilibrium water content and the diffusion coefficient of water in PMMA matrix. Unhydrated blank PMMA samples of known mass and diameter were placed in water. The water uptake by the samples was measured gravimetrically every day for 1 week. The equilibrium water content and the diffusion coefficient were determined from a global two-parameter least-squares fit of the sorption curve for diffusional ingress into a cylinder (19).

NMR Measurements. NMR measurements were made on a Bruker DRX-400 NMR spectrometer with a 1000 G cm^{-1} actively shielded diffusion probe. The measurements were performed at room temperature (23 ± 1 °C). The probe was detuned as a precaution against radiation damping effects. Further details can be found in the literature (20−22).

Longitudinal relaxation times of water protons, T_1, were measured using the standard inversion recovery pulse sequence (23). Transverse relaxation times, T_2, were measured using the standard spin−echo pulse sequence (24) and confirmed using the Carr-Purcell-Meiboom-Gill (CPMG) experiment (180°-pulse spacing 1 ms) (25). The apparent transverse relaxation time, T_2^*, was measured from a least-squares fit of a Lorentzian function to the spectral peak of interest.

Diffusion measurements of water in the microstructure channels were made on the hydrated sample doped with 2.0 mM $CuSO_4$ using the pulsed field gradient spin−echo (PGSE) experiment (26, 27). The measurements were performed in a slice-selective mode in order to contain the region of interest of the PGSE measurement within the probe's constant field-gradient region. An 8-mm thick slice of the sample was selected using a 90° Sinc-7 shaped pulse, which served as the PGSE excitation pulse. The diffusion attenuation of H_2O was measured at a series of values of the diffusion interval, Δ, ranging from 3 to 70 ms. PGSE gradient pulses were sinusoidal and had the duration 0.9 ms. In each measurement, 32 quadratically incremented values of gradient amplitude g were used, resulting in an equidistant spacing of the points in the Stejskal-Tanner plot (21, 22, 28). Diffusion was measured in the direction parallel to the axis of the fiber.

RESULTS AND DISCUSSION

NMR line shapes, relaxation rates, and apparent diffusion coefficients are valuable tools that can be used for characterization of the microstructure and dynamic properties of heterogeneous materials (22, 29−37). Here, we discuss each of these three characteristics of hydrated PMMA optical fibers.

Optical Microscopy. A typical microstructure region of the optical fibers studied is shown in Figure 1c. Some variation in the size of the microstructure channels can be seen, as well as the fact that some channels are situated outside the microstructure region. The latter are attributed to an imperfect bonding between the microstructured preforms and the sleeve in the fiber manufacture process (18). Examination of a number of samples revealed that approximately 99% of channels were $<40\ \mu$m in diameter, with the remaining 1% having diameters $>40\ \mu$m. The latter accounted for ∼1/4 of the total channel volume. The combined cross-sectional area of all channels was (0.4 ± 0.1)% of the cross-sectional area of the fiber. The hexagonally arranged channels shown in Figure 1a comprised approximately half of the total channel volume.

Hydration Measurements. The equilibrium water content in the PMMA samples was found to be (1.3 ± 0.1)% (wt/wt). The diffusion coefficient of water in PMMA, determined from the rate of water ingress into the samples, was 1.2×10^{-12} m^2 s^{-1}. The measured water content is lower than the previously reported value of 2.1% (14), suggesting that the hydration state can vary between PMMA obtained from different manufacturing processes. The measured diffusion coefficient is in qualitative agreement with the results of Rodríguez et al. (38), who reported values in the range from 1.6×10^{-12} to 2.3×10^{-12} m^2 s^{-1}.

NMR Spectra. The NMR spectra of three groups of samples were recorded: hydrated microstructured samples; hydrated blank samples; and a dry (unhydrated) blank sample. The representative spectra are shown in Figure 2. For the hydrated microstructured samples, two NMR peaks were observed. The average separation between the centers of the narrow and the broad peak was 1.53 ppm (610 Hz). Their relative integrals, determined from the nondoped sample, were (25 ± 10)% (narrow peak) and (75 ± 10)% (the broad peak). For the hydrated blank samples, only the broad peak was observed. The spectrum of the dry blank sample, recorded as a control, consisted of the broad peak superimposed on a very broad baseline. The integral of this spectrum was approximately 15% of the broad peak in the hydrated blank sample.

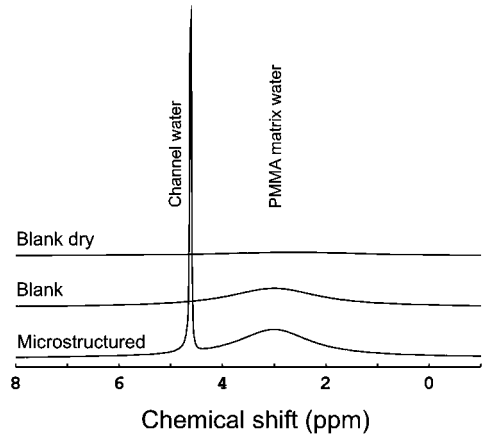

FIGURE 2. NMR spectrum of water in the hydrated microstructured sample, hydrated blank sample and dry blank sample. The integrals of the broad and the narrow peak in the spectrum of the microstructured sample relate approximately as 3:1. The broad peak is attributed to the hydration water of the PMMA matrix; the narrow peak, to the channel water. The spectrum of the dry blank sample consists of the broad peak superimposed on a very broad baseline; it is attributed to a combination of trace water and PMMA methyl groups, as discussed in the text. The integral of the spectrum of the dry blank sample is approximately 15% that of the hydrated blank sample.

The presence of two NMR peaks in the microstructured sample demonstrates the presence of two distinct pools of water molecules in that sample. Conversely, the water in the hydrated blank sample presented as a single pool. The line width of the broad peak in the microstructured samples was similar to that of the peak observed in the hydrated blank sample. We therefore attribute the two peaks to the water absorbed in the polymer matrix (the broad peak) and the water residing in the channels (the narrow peak). The broad peak in the dry blank sample is attributed to the trace water in the polymer; the broad baseline is attributed to the methyl groups of the polymer. The relaxation experiments, which are described below, support these assignments.

The relative populations of the two pools of water in the microstructured sample correspond to the normalized integrals of the respective NMR peaks: 25% for the channel water and 75% for the matrix water. The degree of hydration of the matrix PMMA can be determined from these integrals using the estimated ratio of the volume of the matrix to the volume of the channel space (∼250:1) and the measured density of PMMA ($\rho = 1.19$ g cm^{-3}). The resulting estimate is (1.0 ± 0.3)% (wt/wt) of absorbed water, which is in agreement with the result of the hydration measurements discussed above (1.3%). This water content corresponds to 1 water molecule per every 14−18 monomer units. The low degree of hydration is consistent with the previously reported measurements and with the relatively apolar structure of PMMA.

The observed separation between the two peaks ($\delta\nu$ = 610 Hz) is significant for two reasons. First, it provides the

lower limit for the time scale of chemical exchange between the two pools of water: the exchange time τ must be longer than $1/\pi\delta\nu = 0.5$ ms (39). Second, the chemical shift difference of 1.53 ppm is of interest in its own right. The initial hypothesis was that this difference could be explained in terms of the difference between the magnetic susceptibilities of water and PMMA. The volume magnetic susceptibility of water is −9.05 ppm (SI units) (40). Molar magnetic susceptibility of methyl methacrylate is -57.3×10^{-6} cm^3 mol^{-1} (CGS units) (41). Using the relationship $\chi_V^{SI} = 4\pi\rho\chi_{mol}^{CGS}/MW$, we obtain the SI volume magnetic susceptibility of PMMA of −8.56 ppm. This suggests that the difference between the NMR chemical shifts of PMMA water and channel water should be +0.5 ppm; the observed difference was −1.5 ppm. Therefore, the observed chemical shift difference cannot be explained by the magnetic susceptibilities of water and liquid methyl methacrylate. Unfortunately, a direct comparison with χ of solid PMMA is not possible at this time. The values of magnetic susceptibility of PMMA and similar polymers available in the literature (42) appear to be unreliable because of lack of agreement between different measurement techniques. At present, we cannot offer a reliable explanation of the sign or the magnitude of the observed chemical shift difference.

Relaxation Experiments: Nondoped Samples. The spin−lattice relaxation time (T_1), measured in the inversion−recovery experiments, characterizes the return of nuclear magnetization to equilibrium following an excitation or an inversion by a radio frequency (RF) pulse. In the dry blank sample, the inversion recovery curve was biexponential: the slow component had the $T_1 = 0.8 \pm 0.1$ s and the relative amplitude ~70%; the fast component had a very short $T_1 < 0.01$ s and the relative amplitude ~30%. The latter component was excluded in the T_1 measurement of all hydrated samples (both blank and microstructured) by excluding the first few points of the inversion recovery curve. For the hydrated, nondoped microstructured sample, the T_1 of the broad peak was found to be 0.823 ± 0.003 s, and for the narrow peak, 2.83 ± 0.06 s. For the hydrated, nondoped blank sample, the broad peak had $T_1 = 0.771 \pm 0.001$ s.

The proton T_1 values of water in hydrated materials and tissues are normally shorter than the T_1 of bulk water at the equivalent measurement conditions (37, 43−48). This is usually due to one or a combination of two factors: (1) the local microscopic viscosity experienced by the water molecules tends to be higher in hydrated materials than in bulk water; (2) in hydrated materials, the observed $R_1 = 1/T_1$ of water is a weighted-average of two pools, "free" water (low R_1, long T_1) and "bound" hydration water (high R_1, short T_1) (49). Low water content tends to be associated with a high proportion of the "bound" water and, consequently, a large average R_1. It is therefore expected that water residing in the polymer matrix should exhibit a shorter T_1 than water residing in the channels. In the microstructured sample, the long T_1 (2.83 s) exhibited by the narrow NMR peak is close to that of bulk water. On the other hand, the shorter T_1 value (0.823 s) exhibited by the broad peak is consistent with the relatively slowly tumbling water molecules residing in the polymer matrix. The single NMR peak exhibited by the hydrated blank sample ($T_1 = 0.771$ s) is consistent with the presence of the hydration water in the PMMA matrix and the absence of slow-relaxing channel water in that sample. In the dry blank sample, the relatively slow-relaxing (0.8 s) signal component was attributed to trace hydration water (most probably absorbed from the atmosphere). The fast-relaxing signal component (<0.01 s) in the dry blank sample was attributed to the methyl groups of the polymer. The contribution of this component to the integral of the broad peak in the spectra of hydrated samples is estimated as <5%. The methyl group signal did not affect the determination of the T_1 values of the water peaks because, after the elimination of the first few inversion−recovery points, it translated into a uniform shift of the inversion−recovery curve.

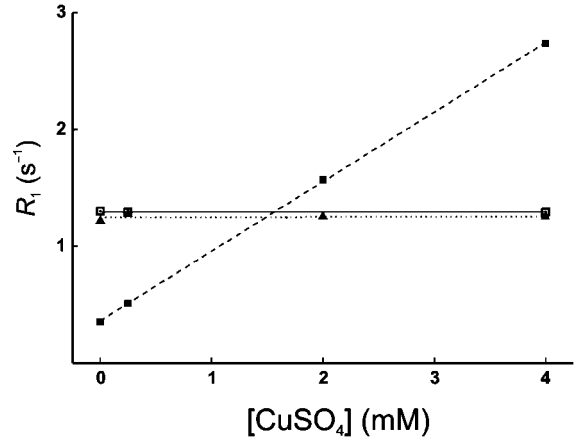

FIGURE 3. Relaxation rates of water in samples doped with $CuSO_4$ solutions. ■, dashed line: microstructured sample, channel water (narrow peak); ▲, dotted line: microstructured sample, matrix water (broad peak); □, solid line: blank sample (only the broad peak was observed). The lines represent linear regression on the respective data point sets. The small difference between the T_1 values of the broad peak in the blank, and the microstructured sample is due to two different batches of PMMA used.

We have examined the possibility that relaxation of water protons could have been affected by the relaxivity of the channel walls. If this were the case, the channel water should have exhibited a distribution of T_1 values determined by the underlying distribution of channel diameters (and surface-to-volume ratios). However, the observed longitudinal relaxation decays of the narrow peak were strictly monoexponential. This suggests that the relaxation behavior of water protons was unaffected by the relaxivity of the channel walls or the size of the host channels.

Relaxation Experiments: Doped Samples. The results of the T_1 measurements for the $CuSO_4$-doped samples are summarized in Figure 3. The proton spin−lattice relaxation rate, R_1, is independent of the concentration of Cu^{2+} for the matrix water (the broad peak) but exhibits a linear dependence on [Cu^{2+}] for the water in the microstructure channels (the narrow peak). The latter effect is well-known (17) and explained by rapid chemical exchange between "free" water and water bound to the paramagnetic Cu^{2+} ion, which acts as a relaxation agent. The resulting contribution to the average relaxation rate of water is linearly proportional

to the concentration of Cu^{2+}. The observed linear relationship between R_1 of the narrow peak and the concentration of $CuSO_4$ demonstrates that the Cu^{2+} ions enter freely into the microstructure channels and their concentration in the channels equals that in the surrounding solution. At the same time, the independence of the R_1 of the broad peak of the concentration of $CuSO_4$ shows that the Cu^{2+} ion is completely excluded from the polymeric matrix of the fiber. The mechanism of this exclusion could be either thermodynamic (high repulsion between Cu^{2+} and the polymer) or kinetic (extremely slow diffusion of Cu^{2+} through the polymer matrix). The kinetic mechanism could be understood intuitively in terms of the very low degree of hydration of the matrix PMMA (one water molecule per 14−18 monomer units). The T_1 values of the broad peak in selected samples were remeasured 6 months later and found to be unchanged. Whether the exclusion of Cu^{2+} from PMMA is thermodynamic or kinetic, its absence from the polymer matrix after such a long period of doping demonstrates that, in practical terms, the matrix is impermeable to Cu^{2+}.

Figure 3 also reveals a systematic and constant difference between the T_1 values of the matrix water in the blank and the microstructured samples. This is consistent with the PMMA used for the two types of samples originating from two different manufacturers and could be attributed to a small difference in the polymer density between the two batches used. Nevertheless, the difference between the T_1 values is small and suggests that the hydration state of the PMMA matrix is similar in the two types of samples.

The spin−spin relaxation time values, T_2, measured for the broad peak of the microstructured sample doped with 2 mM $CuSO_4$, were (0.47 ± 0.01) ms from CPMG measurements (CP time 0.5 ms) and (0.465 ± 0.005) ms from SE measurements (echo time up to 5 ms). The fact that the two measured T_2 values were within the standard measurement error of each other is consistent with the absence of a millisecond-time scale exchange between the channel and the matrix water. The short T_2 values of the broad NMR peak are consistent with the relatively high effective viscosity of the polymer and, consequently, low reorientational mobility of the hydration water residing in the PMMA matrix.

The apparent transverse relaxation time, T_2*, of the same peak in the same sample was found to be 0.476 ms. The fact that the measured T_2 and T_2* were within the measurement error of each other shows that homogeneous contributions to the line shape of the broad peak were negligible. This suggests the polymer density was approximately uniform across the sample. This conclusion is consistent with the strictly monoexponential relaxation of the matrix water.

Diffusion Measurements. Diffusion of molecules such as water can be measured by the pulsed-field gradient spin−echo experiment (29), which is sensitive to both random (diffusion) and coherent (flow) displacement (50, 51). Diffusion in a confined space, where only a fraction of the entire 3D volume is accessible to a diffusing species, is referred to as restricted diffusion. Restricted diffusion is generally characterized by an apparent diffusion coefficient

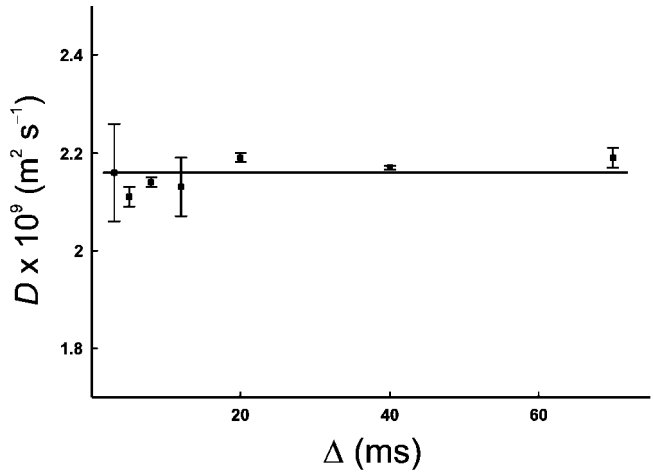

FIGURE 4. Apparent self-diffusion coefficient of the channel water in the direction of the axis of the fiber as a function of the diffusion time. The solid horizontal line corresponds to the average value of D (2.16×10^{-9} m^2 s^{-1}) and is given as a visual guide. Within the standard error of the measurement, the apparent D is independent of Δ.

D_{app}, which depends on the diffusion time Δ (31). At $\Delta \rightarrow 0$, D_{app} approaches the unrestricted D in the bulk solution (D_0). In the limit $\Delta \rightarrow \infty$, D_{app} approaches the asymptotic value D_0/T, where T is the tortuosity of the pore space.

The observed self-diffusion coefficient of water in the microstructure channels of the sample doped with 2 mM $CuSO_4$ is plotted in Figure 4 as a function of the diffusion time. The values of the diffusion coefficient are unchanging within error over a range from 3 to 70 ms. The average value of D is 2.16×10^{-9} m^2 s^{-1}. This is within the standard error of the accepted literature value of D for water: 2.19×10^{-9} at 23 °C (52). This suggests that neither the adsorption of water molecules on the channel walls nor the presence of 2.0 mM $CuSO_4$ had an appreciable effect on the value of D. This finding is expected, as at $[Cu^{2+}] = 2.0$ mM, only ∼0.02 % of all water molecules are coordinated to Cu^{2+} at any given time. The fraction of water molecules adsorbed on the channel walls depends on the surface-to-volume ratio of the channels, but is also expected to be very small in light of the relaxation results discussed above.

The absence of a measurable dependence of the observed D on the diffusion time demonstrates that the diffusion of water along the axial direction of the MPOF was unhindered on the length scale of at least hundreds of microns. The fact that the measured and the literature D are equal (within the measurement error) shows that the water residing in the microstructure channels has the same effective viscosity as the bulk water. It also demonstrates that there is no appreciable exchange between the channel and the matrix water on the time scales shorter than ∼100 ms.

MPOFs in Potential Chemical-Sensor Applications. The finding that charged ions are confined to the microstructure channels and do not enter the polymer matrix is promising in the context of using MPOFs as chemical sensors. Although the tests were conducted only for the Cu^{2+} ion, we expect the findings to be similar for other charged species with comparable or larger ionic radii.

The fact that ionic species do not enter the polymer matrix suggests that PMMA optical fibers are likely to be resistant to degradation associated with the ingress of such species into the polymer matrix, and for the fiber probes to be reusable. It also suggests that ionic species in the microstructure channels can be rapidly exchanged, making MPOFs suitable for real-time monitoring of the properties of an ionic aqueous solution.

The absence of a fast exchange between the channel and the matrix water is consistent with the low diffusion coefficient of the matrix water (1.2×10^{-12} m^2 s^{-1}). A considerable time is required for the hydration water to diffuse into the PMMA matrix: for example, at the diffusion time of 1 h the rms displacement of water in PMMA is only 120 μm. A practical implication of this is that PMMA matrix of MPOFs may need to be "prehydrated" prior to their immediate use.

CONCLUSIONS

This work is the first NMR study characterizing the physical state and dynamics of water in hydrated microstructured polymer optical fibers, or indeed microstructured optical fibers made of any material. The NMR spectra and relaxation measurements unambiguously show the presence of two distinct pools of water in hydrated MPOFs. Water residing in the microstructure channels (approximately 25% of all water) exhibits the molecular mobility similar to that of bulk water. The hydration water residing in the polymer matrix of the fiber (75%) is relatively immobile. The chemical shift difference between the two water peaks is unexpectedly large (1.53 ppm) and cannot be explained by the magnetic susceptibilities of water and liquid methyl methacrylate. This calls for further research into the state of hydration water in PMMA. The exchange between the two populations is slow on the NMR time scale and appears to be limited by the diffusion of water through the polymeric matrix, rather than the size of the microstructure channels. Monoexponential NMR relaxation exhibited by both water pools suggests that the PMMA density was uniform across the sample, and that the mobility of the channel water was unaffected by the diameter of the host channel. As demonstrated by the relaxation measurements of the fibers doped with copper sulfate, charged species enter the microstructure channels freely but are excluded from the polymer matrix of the fiber. The diffusional motion of the channel water along the axial direction of the fiber is unimpeded on the length scale of at least hundreds of micrometers. The methodology presented comprises a robust and general approach to characterization of the physicochemical state of water in polymer optical fibers and will complement the more traditional structural characterization techniques. The findings also suggest that microstructured PMMA optical fibers are suitable for chemical-sensing applications involving ionic aqueous solutions.

Acknowledgment. The authors acknowledge Dr. Maryanne Large (OFTC, Sydney) for providing the facilities for the preparation of optical fiber samples and postgraduate supervision of F.M.C.

ABBREVIATIONS AND SYMBOLS

CPMG, Carr–Purcell–Meiboom–Gill experiment
D, diffusion coefficient
LSF, least-squares fit
MPOF, microstructured polymer optical fiber
NMR, nuclear magnetic resonance
PGSE, pulsed field gradient spin echo
PMMA, poly(methyl methacrylate)
R_1, longitudinal relaxation rate constant
T_1, longitudinal relaxation time constant
T_2, transverse relaxation time constant
T_2*, apparent transverse relaxation time constant
Δ, diffusion time
$\delta\nu$, separation between spectral peaks (Hz)
$\Delta\nu_{1/2}$, line width at half-height (Hz)
ρ, density of PMMA
χ, magnetic susceptibility

REFERENCES AND NOTES

(1) Knight, J. C. *Nature* **2003**, *424*, 847–851.
(2) Hoo, Y. L.; Jin, W.; Ho, H. L.; Wang, D. N.; Windeler, R. S. *Opt. Eng.* **2002**, *41*, 8–9.
(3) Ritari, T.; Tuominen, J.; Ludvigsen, H.; Petersen, J. C.; Sorensen, T.; Hansen, T. P.; Simonsen, H. R. *Opt. Express* **2004**, *12*, 4080–4087.
(4) Cox, F. M.; Argyros, A.; Large, M. C. J. *Opt. Express* **2006**, *14*, 4135–4140.
(5) Cox, F. M.; Lwin, R.; Large, M. C. J.; Cordeiro, C. M. B. *Opt. Express* **2007**, *15*, 11843–11848.
(6) Jensen, J. B.; Hoiby, P. E.; Emiliyanov, G.; Bang, O.; Pedersen, L. H.; Bjarklev, A. *Opt. Express* **2005**, *13*, 5883–5889.
(7) Large, M. C. J.; Argyros, A.; Cox, F.; van Eijkelenborg, M. A.; Ponrathnam, S.; Pujari, N. S.; Bassett, I. M.; Lwin, R.; Barton, G. W. *Mol. Cryst. Liq. Cryst.* **2006**, *446*, 219–231.
(8) Emiliyanov, G.; Jensen, J. B.; Bang, O.; Hoiby, P. E.; Pedersen, L. H.; Kjaer, E. M.; Lindvold, L. *Opt. Lett.* **2007**, *32*, 460–462.
(9) Jean, Y. C.; Nakanishi, H.; Hao, L. Y.; Sandreczki, T. C. *Phys. Rev. B* **1990**, *42*, 9705–9708.
(10) Weisenberger, L. A.; Koenig, J. L. *Macromolecules* **1990**, *23*, 2445–2453.
(11) Hyde, T. M.; Gladden, L. F.; Mackley, M. R.; Gao, P. *J. Polym. Sci.: Polym. Chem.* **1995**, *33*, 1795–1806.
(12) Thomas, N.; Windle, A. H. *Polymer* **1978**, *19*, 255–265.
(13) Large, M. C. J.; Ponrathnam, S.; Argyros, A.; Pujari, N. S.; Cox, F. *Opt. Express* **2004**, *12*, 1966–1971.
(14) Kusy, R. P.; Whitley, J. Q.; Kalachandra, S. *Polymer* **2001**, *42*, 2585–2595.
(15) Probstein, R. F. *Physicochemical Hydrodynamics: An Introduction*; John Wiley & Sons, Inc.: Hoboken, NJ, 2005.
(16) Banci, L.; Bertini, I.; Luchinat, C. *Nuclear and Electronic Relaxation*; VCH: Weinheim, Germany, 1991.
(17) Lauffer, R. B. *Chem. Rev.* **1987**, *87*, 901–927.
(18) Barton, G.; van Eijkelenborg, M. A.; Henry, G.; Large, M. C. J.; Zagari, J. *Opt. Fiber Technol.* **2004**, *10*, 325–335.
(19) Crank, J. *The Mathematics of Diffusion*, 2nd ed.; Clarendon Press: Oxford, U.K., 1975.
(20) Momot, K. I.; Kuchel, P. W.; Chapman, B. E.; Deo, P.; Whittaker, D. *Langmuir* **2003**, *19*, 2088–2095.
(21) Momot, K. I.; Kuchel, P. W. *J. Magn. Reson.* **2004**, *169*, 92–101.
(22) Regan, D. G.; Momot, K. I.; Martens, P. J.; Poole-Warren, L. A.; Kuchel, P. W. *Diffus. Fundam.* **2006**, *4*, 1.1–1.18.
(23) Vold, R. L.; Waugh, J. S.; Klein, M. P.; Phelps, D. E. *J. Chem. Phys.* **1968**, *48*, 3831–3832.
(24) Hahn, E. L. *Phys. Rev.* **1950**, *80*, 580–594.
(25) Meiboom, S.; Gill, D. *Rev. Sci. Instrum.* **1958**, *29*, 688–691.
(26) Stejskal, E. O.; Tanner, J. E. *J. Chem. Phys.* **1965**, *42*, 288–292.
(27) Johnson, C. S. *Prog. Nucl. Magn. Reson. Spectrosc.* **1999**, *34*, 203–256.
(28) Momot, K. I.; Kuchel, P. W.; Chapman, B. E. *J. Magn. Reson.* **2005**, *176*, 151–159.
(29) Callaghan, P. T. *Principles of Nuclear Magnetic Resonance Microscopy*; Clarendon Press: Oxford, U.K., 1991.

(30) Blümich, B. *NMR Imaging of Materials*; Claredon Press: Oxford, U.K., 2000.
(31) Mitra, P. P.; Sen, P. N.; Schwartz, L. M.; Ledoussal, P. *Phys. Rev. Lett.* **1992**, *68*, 3555–3558.
(32) McConville, P.; Pope, J. M. *Polymer* **2000**, *41*, 9081–9088.
(33) Silva, C. L.; Topgaard, D.; Kocherbitov, V.; Sousa, J. J. S.; Pais, A.; Sparr, E. *Biochim. Biophys. Acta, Biomembr.* **2007**, *1768*, 2647–2659.
(34) Aslund, I.; Cabaleiro-Lago, C.; Soderman, O.; Topgaard, D. *J. Phys. Chem. B* **2008**, *112*, 2782–2794.
(35) Dvoyashkin, M.; Valiullin, R.; Karger, J.; Einicke, W. D.; Glaser, R. *J. Am. Chem. Soc.* **2007**, *129*, 10344–10345.
(36) de Visser, S. K.; Bowden, J. C.; Wentrup-Byrne, E.; Rintoul, L.; Bostrom, T.; Pope, J. M.; Momot, K. I. *Osteoarthr. Cartilage* **2008**, *16*, 689–697.
(37) Momot, K. I.; Takegoshi, K.; Kuchel, P. W.; Larkin, T. J. *J. Phys. Chem. B* **2008**, *112*, 6636–6645.
(38) Rodriguez, O.; Fornasiero, F.; Arce, A.; Radke, C. J.; Prausnitz, J. M. *Polymer* **2003**, *44*, 6323–6333.
(39) Sandstroem, J. *Dynamic NMR Spectroscopy*; Academic Press: London, 1982.
(40) Doty, F. D.; Entzminger, G.; Yang, Y. A. *Concepts Magn. Reson.* **1998**, *10*, 133–156.
(41) *CRC Handbook of Chemistry and Physics*, 88th ed.; Lide, D. R., Ed.; CRC Press: Boca Raton, FL, 2007.
(42) Tanimoto, Y.; Fujiwara, M.; Sueda, M.; Inoue, K.; Akita, M. *Jpn. J. Appl. Phys., Part 1* **2005**, *44*, 6801–6803.
(43) Baumgartner, S.; Lahajnar, G.; Sepe, A.; Kristl, J. *Eur. J. Pharm. Biopharm.* **2005**, *59*, 299–306.
(44) Blinc, A.; Lahajnar, G.; Blinc, R.; Zidansek, A.; Sepe, A. *Magn. Reson. Med.* **1990**, *14*, 105–122.
(45) Jones, C. E.; Pope, J. M. *Magn. Reson. Imaging* **2004**, *22*, 211–220.
(46) McConville, P.; Whittaker, M. K.; Pope, J. M. *Macromolecules* **2002**, *35*, 6961–6969.
(47) Jones, C. E.; Atchison, D. A.; Meder, R.; Pope, J. M. *Vision Res.* **2005**, *45*, 2352–2366.
(48) Koenig, S. H.; Brown, R. D., III; Adams, D.; Emerson, D.; Harrison, C. G. *Invest. Radiol.* **1984**, *19*, 76–81.
(49) Momot, K. I.; Kuchel, P. W. *Concepts Magn. Reson.* **2003**, *19A*, 51–64.
(50) Johnson, C. S. Diffusion Measurements by Magnetic Field Gradient Methods. In *Encyclopedia of Nuclear Magnetic Resonance*; Grant, D. M., Harris, R. K., Eds.; Wiley: New York, 1996; Vol. 3, pp 1626—1644.
(51) Momot, K. I.; Kuchel, P. W. *Concepts Magn. Reson.* **2006**, *28A*, 249–269.
(52) Mills, R. *J. Phys. Chem.* **1973**, *77*, 685–688.

AM800059C